



## Single vs dual source surface energy balance model based actual evapotranspiration estimation

**Richa Pandey**

Water Technology Centre, ICAR-Indian Agricultural Research Institute, New Delhi, India

**Ravinder Kaur** ✉

Water Technology Centre, ICAR-Indian Agricultural Research Institute, New Delhi, India

**Ivo Zution Goncalves**

The Daugherty Water for Food Global Institute, University of Nebraska, Lincoln, USA

**Christopher Neale**

The Daugherty Water for Food Global Institute, University of Nebraska, Lincoln, USA

**Manoj Khanna**

Water Technology Centre, ICAR-Indian Agricultural Research Institute, New Delhi, India

**Man Singh**

Water Technology Centre, ICAR-Indian Agricultural Research Institute, New Delhi, India

**Vinay Kumar Sehgal**

Division of Agricultural Physics, ICAR-Indian Agricultural Research Institute, New Delhi, India

**Arjamadutta Sarangi**

Water Technology Centre, ICAR-Indian Agricultural Research Institute, New Delhi, India

**Manjaiah Kanchikeri Math**

Division of Soil Science and Agricultural Chemistry, ICAR-Indian Agricultural Research Institute, New Delhi, India

### ARTICLE INFO

Received : 10 November 2023

Revised : 28 November 2023

Accepted : 30 November 2023

Available online: 19 January 2024

#### Key Words:

Canal water allocation

Crop water demand mapping

Energy budgeting

Evapotranspiration Flux Modeling

### ABSTRACT

The current study aims to inter-compare the performance efficiency of the single and the dual source surface energy balance modeling approaches, namely EEFlux and SETMI, respectively for real time catchment scale - crop water demand estimations. For this, the afore-stated two surface energy balance modelling approaches were applied on the Narmada Canal Project, Sanchore, Rajasthan, India for estimating catchment scale actual evapotranspiration (ETa) values for the Rabi cropping seasons of the years 2013-14 and 2018-19, after incorporating the basic satellite data derived inputs viz. Land use, Land surface temperature and Gridded weather data. Due to the non-availability of the catchment scale ground based daily reference evapotranspiration (ETo) values for the study area, the Global Land Data Assimilation System based gridded meteorological data product was utilized, as a substitute for obtaining observed actual evapotranspiration (ETa) values for the investigated Rabi seasons of the study area. These actual evapotranspiration values were compared with those estimated through the single source, EEFlux and the dual source, SETMI modelling approaches to ascertain their comparative performance efficiency through the use of the five statistical indices viz. Mean Absolute Error, Root Mean Square Error, Mean Bias Error, Nash-Sutcliffe Efficiency and the Index of Agreement. The investigations revealed almost at par performance of the two modelling approaches. However, it was concluded that in contrast to the more detailed dual source approach i.e., SETMI, the simple single source approach i.e., EEFlux seemed to be more promising due to its user-friendly implementation and input data automation.

### Introduction

India currently ranks 13<sup>th</sup> among the 17 most water-stressed nations, presenting a concerning scenario. The impending impacts of global climate change, leading to a warmer climate, are expected to worsen

Corresponding author E-mail: [ravinder.kaur@icar.gov.in](mailto:ravinder.kaur@icar.gov.in)

Doi: <https://doi.org/10.36953/ECJ.27532611>

This work is licensed under Attribution-Non Commercial 4.0 International (CC BY-NC 4.0)

© ASEA

this water scarcity. This is primarily due to an intensified hydrological cycle caused by rising temperatures, resulting in increased evaporation rates, shifts in precipitation patterns in terms of both intensity and seasonality, and changes in vegetation and land cover dynamics. In India, agriculture sector utilizes about 85% of available water resource followed by 8% and 7% by the domestic and industrial sectors respectively. Canal irrigation, coupled with groundwater, has undeniably played a vital role in accelerating agricultural production of India for meeting burgeoning population needs. Thus, in view of the looming climate change related threats it is likely that any further shortfall in water supply, especially in the already vulnerable arid and semi-arid regions, is likely to intensify the competition for water use across various economic, social, and environmental applications besides food production.

Canal irrigation techniques were originally designed with an intent to minimize disparities in water distribution among various users, however significant shortcomings have emerged in its functioning, primarily due to its reliance on a supply-based, rather than a demand-based system. This has adversely impacted its efficiency and effectiveness, giving rise to several various issues of concern such as uneven water distribution leading to over-irrigation in head reaches and reduced supplies in tail reaches along with inflexible water allocations. To implement an economically equitable water distribution irrigation system, a transition from supply based to near real time demand-based irrigation systems is essential. Accurate estimation of actual evapotranspiration (ET<sub>a</sub>) can play a pivotal role in this shift, as it represents the earth's principal outgoing energy flux related to the water cycle dynamics. Globally, the ET<sub>a</sub> accounts for nearly 60% of the mean precipitation inputs (Vorosmarty *et al.*, 2010) highlighting its significant implications for numerous geophysical applications including integrated water resources management, weather forecasting, climate change analysis, and irrigation water demand assessment. (Dai *et al.*, 2022; Kushwaha *et al.*, 2022; Salam *et al.*, 2020). Point scale field observations offer satisfactory solutions for ET<sub>a</sub> computation over homogenous surfaces. However, extrapolation of these point values over diverse spatial and temporal scales includes several

underlying complexities due to the geographical variability in land surface and environmental conditions (Singh *et al.*, 2008; Teixeira *et al.*, 2009). These issues have been proficiently dealt with regular updates in remote sensing-based methodologies by indirectly quantifying spatially distributed parameters required for ET<sub>a</sub> estimation. Courault *et al.*, (2005) classified remote sensing-based evapotranspiration techniques in four major categories viz. Direct Empirical Methods, Residual Methods of Energy Budget, Deterministic Methods and Inference or Vegetation Index Methods. Amongst these, residual method of energy budget is the most widely used methods for ET<sub>a</sub> determination because of its ease of applicability and readily available remote sensing inputs.

Residual method of energy budget is further classified into single and dual-source model categories based on distinct treatment of the soil-plant-atmosphere interface. The dual-source approaches treat soil as well as vegetation components individually for apportioning linked turbulent heat fluxes while the single-source modeling approaches use individual resistance as a lumped composite parameter. Thus, for homogeneous vegetative conditions, a single-source modeling approach might be suitable. While, under heterogenous partially vegetated conditions, a two-source modelling approach that is capable of more genuine representation of the turbulent and radiation exchanges (Verhoef *et al.*, 1997; Merlin & Chehbouni, 2004; Norman *et al.*, 2000; Huntingford *et al.*, 2000) is expected to replicate the earth's surface energy balance with higher accuracy (Norman *et al.*, 1995). However, despite all this, it has been reported by several researchers that even an appropriately parameterized simple single-source modeling approach may represent surface energy balance satisfactorily (Kustas and Norman, 1996; Troufleau *et al.*, 1997; Bastiaanssen *et al.*, 1998). Though strengths and limitations of various residual methods of energy budget have been extensively reviewed (Gowda *et al.*, 2008; Li *et al.*, 2009; Wang and Dickinson, 2012; Liou and Kar, 2014; Kool *et al.*, 2014; Zang *et al.*, 2016) and mostly validated across irrigated croplands of USA, China, Mongolia, South Korea, and Japan yet scanning of literature revealed almost no assessment of such minimum resource and data demanding approaches on any

resource/ data crunched water scarce regions of the world.

In view of the afore-stated knowledge gaps, the present study thus basically aims to cross-compare the performance efficiency of one of the latest and the most automated data intensive single source energy balance models viz., EEFlux with yet another latest dual source, but data-extensive, energy balance model named SETMI on the country's first sprinkler-fed Narmada Canal Command situated in the arid Rajasthan state of India, and to thereby assess the feasibility of such satellite based approaches for transforming the prevailing supply driven irrigation system to the near real time demand-driven system and for thereby mitigating climate induced water stresses in the resource-poor arid croplands.

## Material and Methods

### Study Area

The Narmada Canal Project (study) area (figure 1), located in the Barmer and Jalore district of Rajasthan, India, within the geographical coordinates of 24° 37'- 25° 18' N latitude and 71° 3'- 71° 52' E Longitude, comprises of 2.46 lakh ha command area. The climate of the region varies from arid to semi-arid as it falls in the two agroclimatic zones namely, the arid western plains and the transitional plains of Luni basin. Due to erratic, unevenly distributed and less than 500 mm annual rainfall along with substantial diurnal temperature variations, the study area experiences frequent crop failures due to droughts.

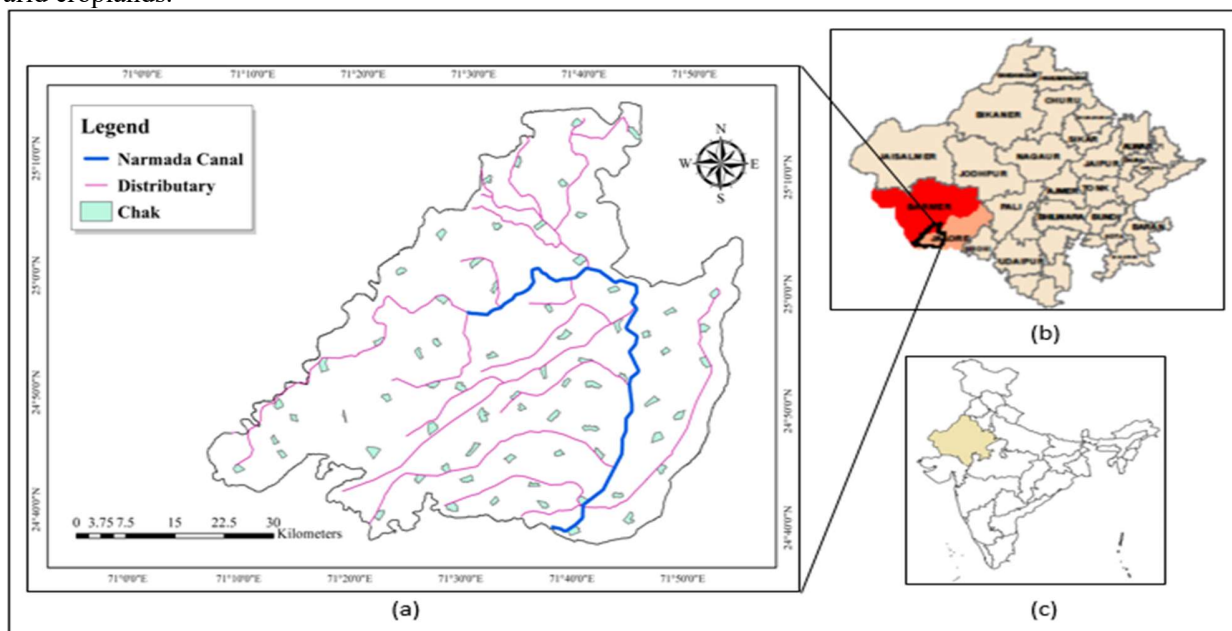


**Figure 1(a): Location map of the study area (b) Study area boundary in Rajasthan state (c) Map showing Rajasthan state boundary within Indian national boundary**

### Modelling approaches for estimating actual evapotranspiration

#### EEFlux model

The Google Earth Engine Evapotranspiration Flux (EEFlux) is an automated version of METRIC (Mapping Evapotranspiration at high Resolution with Internalized Calibration) which is developed and designed within the Google Earth Engine (GEE) (Allen *et al.*, 2007). This software is collaboratively developed by a group of researchers from the Desert

Research Institute, University of Nebraska-Lincoln, and the University of Idaho, with financial assistance provided by the Google. EEFlux enable users to acquire evapotranspiration maps in a matter of seconds using Landsat 5,7 or 8 scenes stored in the GEE cloud platform (Allen *et al.*, 2015). EEFlux utilizes European Space Agency (ESA) GlobCover land use map with an approximate resolution of 300 m for Indian continent. For locations outside the United States, EEFlux utilizes Climate Forecast

System Reanalysis (CFSR) gridded weather data (<http://cfs.ncep.noaa.gov/cfsr/>) (Saha *et al.*, 2010) and six hourly CFSv2 operational analysis (Yuan *et al.*, 2011; Saha *et al.*, 2013). For current study Landsat 8 images were processed on EEFlux version 0.20.3.

#### SETMI model

The Spatial evapotranspiration modeling interface (SETMI) is a hybrid modelling interface (Neale *et al.*, 2012) combining Two Source Energy Balance (TSEB) ET modal (Norman *et al.*, 1995) and a reflectance-based crop coefficient (Kcbrf) water balance modal (Neale *et al.*, 1989). It was developed jointly by collaborators from Utah State University and the University of Nebraska-Lincoln, USA (Geli and Neale, 2012). This interface operates within the ESRI ArcGIS environment and is coded in Visual Basic.NET. In our study, only the TSEB model within the SETMI interface was used for ETa estimation. Required input included multispectral images, radiometric surface temperature images (in °C), land cover classification image and weather parameter table.

#### Model input data generation

The study area could be covered in three Landsat 8 satellite data tiles (having following paths/rows viz., 149/43, 150/43 and 150/42), that were directly downloaded from the <https://earthexplorer.usgs.gov/> website and mosaiced together to achieve a single input image (Figure 2) for the entire study area, for the nearest satellite pass dates. Table 1 illustrates the exact dates for which the afore-stated satellite images were downloaded and mosaiced together for the study area. The so downloaded and mosaiced satellite images for the band Nos. 3, 4, and 5 of the Landsat 8 were subjected to level-1 supervised classification to generate land use/ land cover maps (as illustrated in Figure 3 and 4) under three primary land use classes viz. Cropped area, bare soil and open water while band 10 of Landsat 8 was used for generating the land surface temperature images through ArcGIS software.

Besides these afore-stated inputs, the SETMI model requires instantaneous and daily reference evapotranspiration (ETo) data to scale modelled instantaneous latent heat flux into daily ETa values after having ETo values multiplied with the crop coefficient values for the dominant crop being

cultivated during Rabi season in the study area. However, due to the unavailability of ground based meteorological data for providing instantaneous meteorological parameters and daily ETo at the satellite overpass time for the study area, Global Land Data Assimilation System's gridded meteorological data product namely, GLDAS\_NOAH025\_3H was employed as a substitute. The Global Land Data Assimilation System (GLDAS) is a terrestrial modelling system developed jointly by the NASA Goddard Space Flight Center (GSFC) and National Oceanic and Atmospheric Administration and is available at a spatial and temporal resolution of  $0.25^{\circ} \times 0.25^{\circ}$  and 3 hours from the reference site, <https://ldas.gsfc.nasa.gov>. Thus, the afore-stated three hourly GLDAS data files, in NetCDF format, were downloaded for the Rabi season of the 2013-14 and 2018-19 and executed in a MATLAB script to extract the relevant weather parameters in .xls format to compute ETo values using FAO Penman-Monteith equation (Allen *et al.*, 1998). Thereafter, the instantaneous value of ETo at satellite overpass time were determined by linearly interpolating ETo values available prior and after the satellite overpass time. Lastly, a weather parameter table was prepared as a Microsoft excel spreadsheet, containing instantaneous values of incident solar radiation, air temperature, wind speed, barometric pressure, vapour pressure and instantaneous and daily ETo. A detailed flowchart depicting the afore-stated methodology for estimating ETa through SETMI modelling framework is illustrated in figure 5.

As per the NCP's detailed project report, the study area has been reported to be predominantly cultivated with Cumin (*Cuminum cyminum*), having an average crop duration of 120-130 days, during Rabi season. Figure 6 illustrates growth stage specific crop coefficient (Kc) values for the Cumin crop. Thus, for computing the observed ETa values, the aforementioned crop coefficient values were multiplied by the ETo values computed through FAO Penman-Monteith equation using GLDAS datasets. The so obtained ETa values (i.e., the observed ETa) were compared with the SETMI and EEFlux model estimated ETa values (i.e., the predicted ETa) to assess their performance efficiency in terms of the following five statistical indices as illustrated in Table 2.

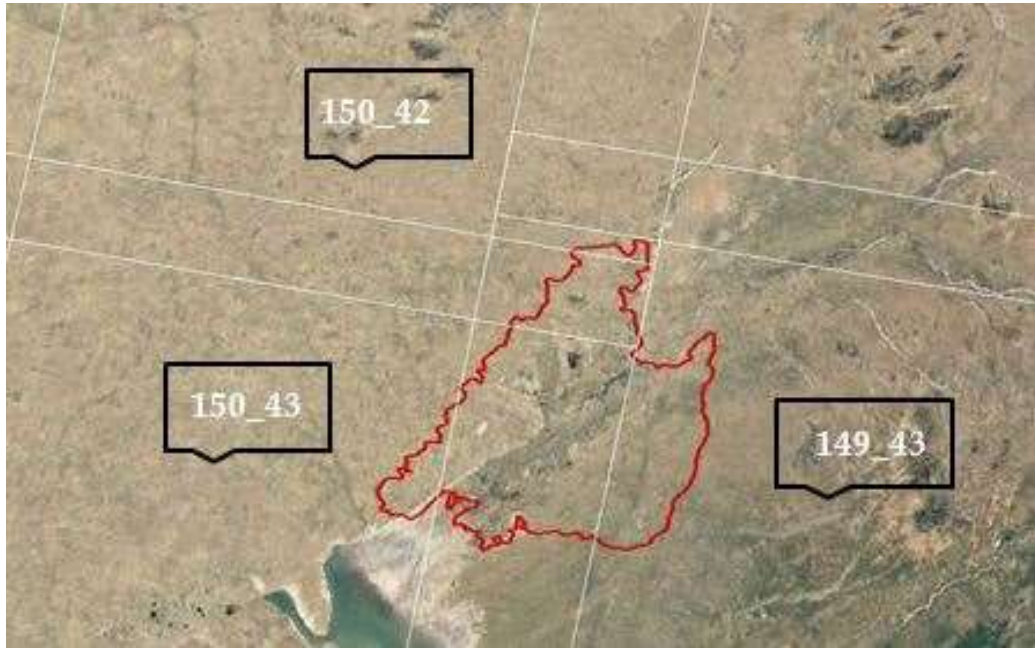


Figure 2: Mosaiced Landsat 8 satellite images for the study area

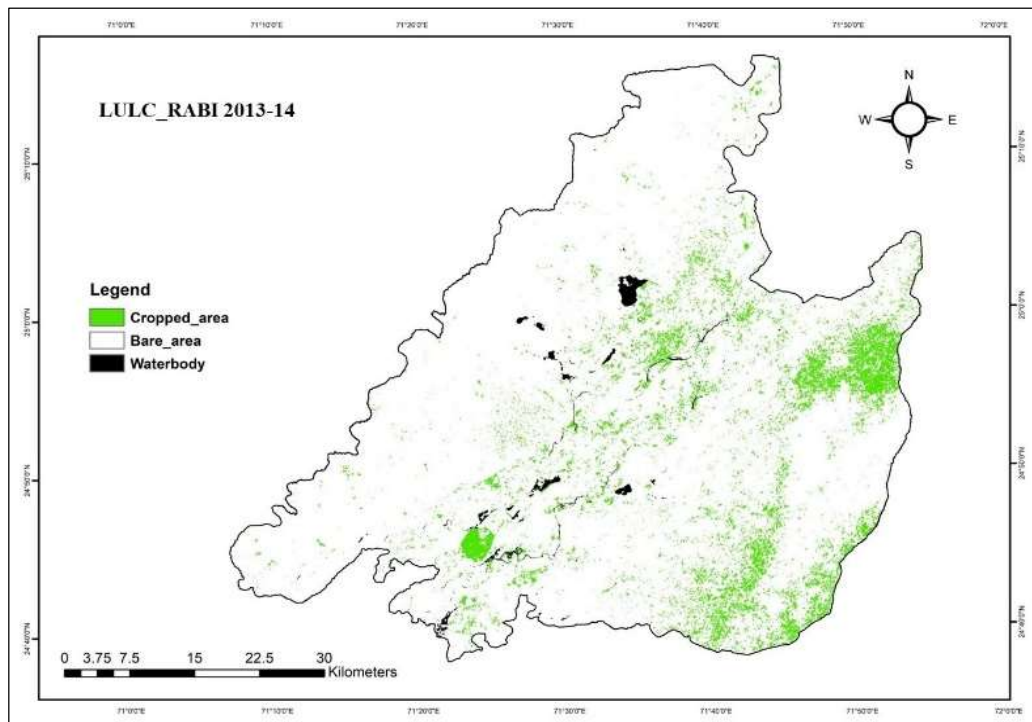


Figure 3: Representative land use/land cover map of study area during Rabi season (2013-14)

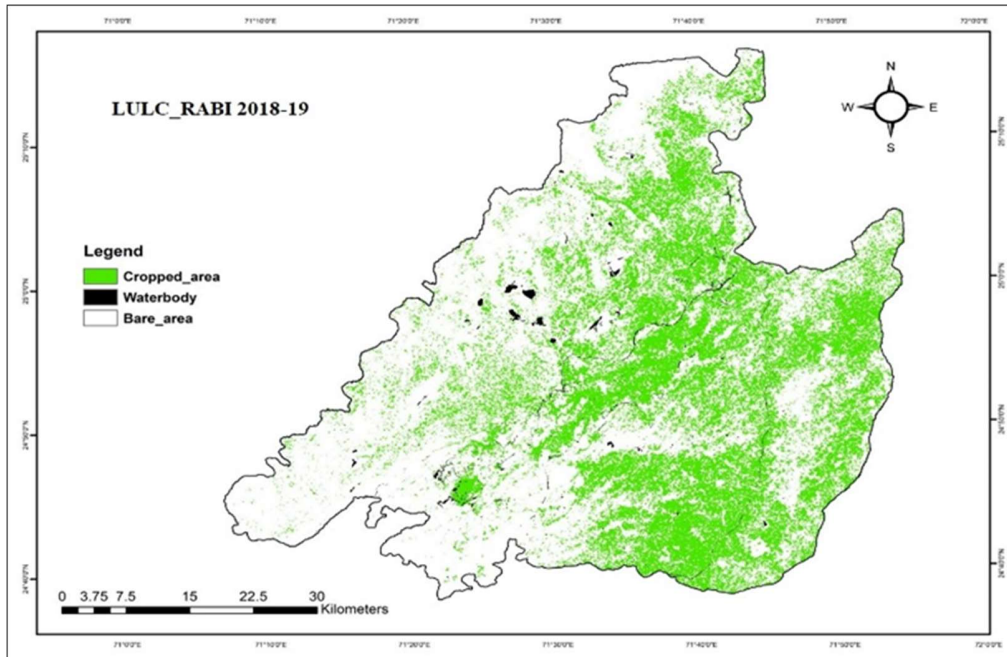


Figure 4: Representative land use/land cover map of study area during Rabi season (2018-19) model performance assessment

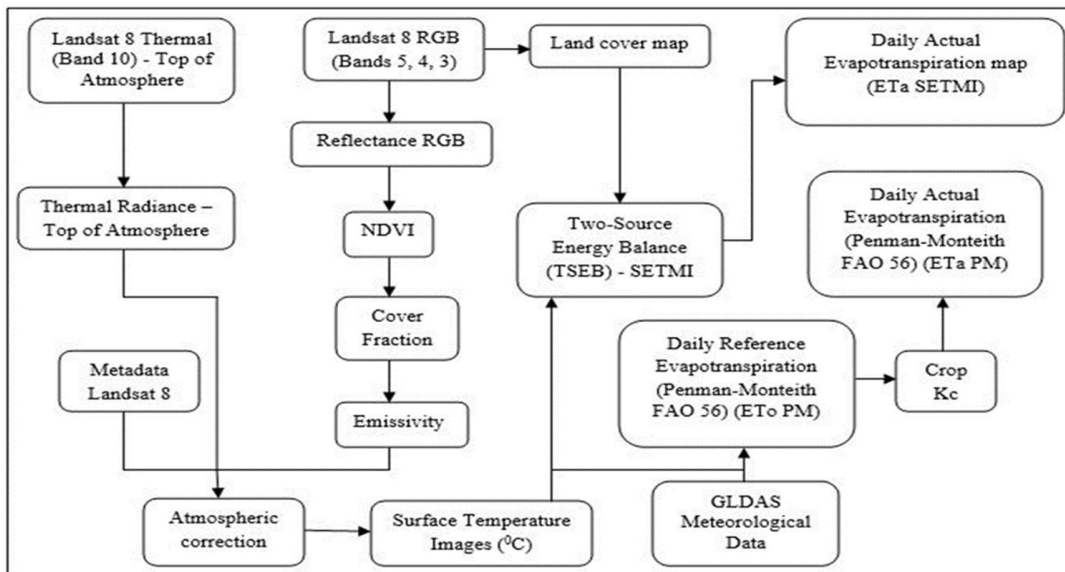


Figure 5: Flow chart depicting methodology used in actual evapotranspiration (ETA) estimation using SETMI model

The Mean Bias Error (MBE) was employed to assess the tendency of the model to under or over-predict. Though, a value of zero denotes no bias but it need not necessarily represent an error absence. Thus, besides MBE, Mean Absolute Error (MAE) and the

Root Mean Square Error (RMSE) were also deployed to not only determine the average errors, irrespective of their directions, in the model prediction sets but to also quantify their spread. Nash-Sutcliffe efficiency (NSE), a normalized

**Table 1: Path/ Row specific dates of the downloaded Landsat 8 images during crop growing season for the study area**

| Crop growth stage specific downloaded Images | Rabi season 2013-2014 (15 <sup>th</sup> Nov – 15 <sup>th</sup> Mar) |            |            | Rabi season 2018-2019 (15 <sup>th</sup> Nov – 15 <sup>th</sup> Mar) |            |            |
|----------------------------------------------|---------------------------------------------------------------------|------------|------------|---------------------------------------------------------------------|------------|------------|
|                                              | 149/43                                                              | 150/43     | 150/42     | 149/43                                                              | 150/43     | 150/42     |
| Initial                                      | 26-11-2013                                                          | 17-11-2013 | 17-11-2013 | 24-11-2018                                                          | 01-12-2018 | 01-12-2018 |
| Vegetative                                   | 12-12-2013                                                          | 03-12-2013 | 03-12-2013 | 26-12-2018                                                          | 02-01-2019 | 02-01-2019 |
| Mid-season                                   | 28-12-2013                                                          | 19-12-2013 | 19-12-2013 | 11-01-2019                                                          | 18-01-2019 | 18-01-2019 |
| Late-season                                  | 02-03-2014                                                          | 09-03-2014 | 09-03-2014 | 27-01-2019                                                          | 03-02-2019 | 03-02-2019 |
| Late-season                                  | -                                                                   | -          | -          | 28-02-2019                                                          | 07-03-2019 | 07-03-2019 |

\* Images for the dates illustrated in each row under columns marked Rabi season (2013-14 and 2018-19) were mosaiced together to generate a single image of the study area

**Table 2: Description for various statistical indices used for model performance assessment**

| Statistic                    | Mathematical Expression                                                                           | Range                                             | Best |
|------------------------------|---------------------------------------------------------------------------------------------------|---------------------------------------------------|------|
| Mean Bias Error              | $MBE = (1/N) \sum_{i=1}^N (P_i - O_i)$                                                            | $-[(\frac{1}{N}) \sum_{i=1}^N (O_i)]$ to $\infty$ | 0    |
| Root Mean Square Error       | $RMSE = \sqrt{(1/N) \sum_{i=1}^N (P_i - O_i)^2}$                                                  | 0 to $\infty$                                     | 0    |
| Mean Absolute Error          | $MAE = (1/N) \sum_{i=1}^N  P_i - O_i $                                                            | 0 to $\infty$                                     | 0    |
| Nash Sutcliffe Efficiency    | $NSE = 1 - [\frac{\sum_{i=1}^N (P_i - O_i)^2}{\sum_{i=1}^N (O_i - \bar{O})^2}]$                   | $-\infty$ to 1                                    | 1    |
| Index of Agreement (d-index) | $d = 1 - [\frac{\sum_{i=1}^N (O_i - P_i)^2}{\sum_{i=1}^N ( P_i - \bar{P}  +  O_i - \bar{O} )^2}]$ | 0 to 1                                            | 1    |

P<sub>i</sub> = Predicted ET<sub>a</sub>; O<sub>i</sub> = Observed ET<sub>a</sub>; P,  $\bar{O}$  = Mean of predicted and observed ET<sub>a</sub> respectively; N = Total number of data record

**Table 3: Catchment scale mean observed vs. predicted ET<sub>a</sub> of the agricultural areas in Narmada Canal Project during (2013-14) Rabi season**

| Date       | Crop Growth Stage | GLDAS_ET <sub>0</sub> | Kc   | GLDAS_ET <sub>a</sub> | EEFlux_ET <sub>a</sub> (mm/d) |      | SETMI_ET <sub>a</sub> (mm/d) |      |
|------------|-------------------|-----------------------|------|-----------------------|-------------------------------|------|------------------------------|------|
|            |                   |                       |      |                       | mean                          | σ    | mean                         | σ    |
| 26/11/2013 | Initial           | 3.56                  | 0.48 | 1.71                  | 1.59                          | 0.61 | 2.88                         | 0.69 |
| 12/12/2013 | Vegetative        | 3.47                  | 1    | 3.47                  | 2.4                           | 0.79 | 2.38                         | 0.43 |
| 28/12/2013 | Mid-season        | 3.38                  | 1.12 | 3.79                  | 4.38                          | 1.49 | 2.97                         | 0.94 |
| 02/03/2014 | Late-season       | 4.58                  | 0.4  | 1.83                  | 2.21                          | 0.71 | 3.32                         | 1.07 |

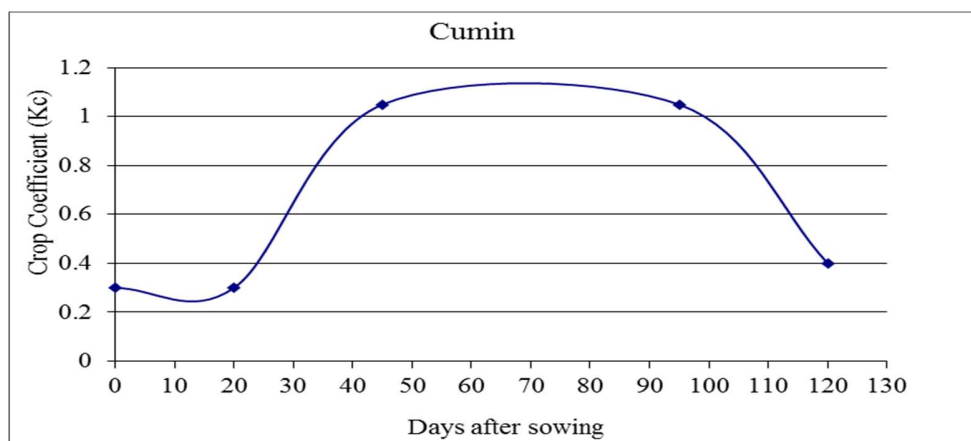


**Figure 6: Seasonal crop coefficient values for Cumin (*Cuminum cyminum*) crop**

statistical index was also utilized to evaluate the predictive capability of the model. Positive values of NSE indicate an acceptable performance level while negative values designate unsatisfactory performance (Nash and Sutcliffe, 1970; Moriasi *et al.*, 2007). However, as NSE is particularly sensitive

to high peaks therefore another index of agreement (d-index) that quantifies the prediction error between 0 and 1 was also applied. The mathematical expressions for all these statistical indices are provided in Table 2.

## Results and Discussion

### Seasonal trend of EEFlux estimated actual evapotranspiration

The ET<sub>a</sub> values estimated through EEFlux modelling approach (EEFlux-ET<sub>a</sub>) during the Rabi season of 2013-14 (Table 3) exhibited considerable variation, ranging from the lowest value of 1.59 mm/d (with a standard deviation,  $\sigma$  of 0.61 mm/d) during initial crop growth stage (i.e., on 11-26-2013) to the highest value of 4.38 mm/d (with  $\sigma$  of 1.49 mm/d) during mid-crop growth stage (i.e., on 12-28-2013). The lower ET<sub>a</sub> observed during the initial crop growth stage could be attributed to smaller leaf areas and limited transpiration rates while, as the crop matured and advanced through its developmental stages, the ET<sub>a</sub> values gradually increased, reaching their peak during the mid-crop growth stage. This escalation could be lucidly attributed to the increased transpiration due to increased crop growth and ground coverage, which eventually reached its maximum during the mid-crop growth stage. Subsequently, with the onset of the late-crop growth stage, there was a gradual decline in ET<sub>a</sub> primarily due to the crop maturity and the prevailing dry soil conditions. The seasonal ET<sub>a</sub> trend of estimated through the EEFlux model during the Rabi season 2013-14 was thus observed to completely conform to the widely accepted pattern of ET<sub>a</sub> dynamics during any crop growing season. Similarly, during the Rabi season of 2018-19 (Table 4), the EEFlux model computed ET<sub>a</sub> values were observed to be ranging from the lowest value of 0.92 mm/d (with  $\sigma$  of 0.74 mm/d) during initial crop growth stage to the highest value of 2.43 mm/d (with  $\sigma$  of 1.47 mm/d) during late-crop growth stage. However, during 2018-19 Rabi season the ET<sub>a</sub> values during mid-crop growth stage were observed to be significantly lower than those observed during the late-crop growth stage of the year 2018-19 primarily due to the desert locust (*Schistocerca gregaria*) attack during Rabi season of the 2018-19, as reported by the local farmers and authorities of the study area which resulted in significant decline in the overall crop cover and thus ET<sub>a</sub> of the study area.

### Seasonal trend of SETMI estimated actual evapotranspiration

In contrast to the EEFlux model the SETMI estimated ET<sub>a</sub> (SETMI\_ET<sub>a</sub>) values exhibited

significant deviations from the general trend of widely accepted pattern of ET<sub>a</sub> dynamics during any crop growing season as these were observed to be the highest during late crop growth stage (3.32 mm/d with  $\sigma$  of 1.07 mm/d) and the lowest (2.38 mm/d with  $\sigma$  of 0.43 mm/d) during crop vegetative stage. Even for the subsequent Rabi season of 2018-19, the SETMI model predicted the highest ET<sub>a</sub> value (2.21 mm/d with  $\sigma$  0.67 mm/d) for the initial crop growth stage and the lowest value for the late crop growth stage (ET<sub>a</sub> of 1.4 mm/d and  $\sigma$  0.63 mm/d). Further, even the mid-season SETMI predicted ET<sub>a</sub> value was observed to be lower than that for the late crop growth stage (1.86 mm/d with 0.74 mm/d). Though this decrease can presumably be attributed to the incident desert locust attack during that season/ year yet it appeared to be also associated to perhaps the poor parameterization of the TSEB algorithm within the SETMI interface, specifically during the initial and the late crop growth stages as evident from the SETMI estimated ET<sub>a</sub> trend for the Rabi season of 2013-14.

### Observed vs predicted actual evapotranspiration

Figures 7 and 8 illustrate observed (i.e., GLDAS\_ET<sub>a</sub>, in mm/d) vs. predicted actual evapotranspiration rates (Modelled\_ET<sub>a</sub>, in mm/d) as obtained through the EEFlux (EEFlux\_ET<sub>a</sub>, Table 3 and 4) and the SETMI models (SETMI\_ET<sub>a</sub>, Table 3 and 4) for the Rabi seasons of (2013-14) and (2018-19), respectively. While for assessing the comparative performance efficiency of the two modelling approaches, the afore-generated data were subjected to the statistical indices illustrated in Table 5. Cross comparison of these statistical index values revealed that the EEFlux model seemed to be associated with much lower RMSE values (0.64 mm/d) than the SETMI model (1.17 mm/d), during 2013-14 while SETMI model seemed to be associated with much lower RMSE values (1.83 mm/d) than the EEFlux model (2.04 mm/d), during 2018-19. However, on considering all data points for both the study periods/ seasons, the RMSE values for both the modelling approaches were found to be at par (i.e., 1.57 to 1.58 mm/d). Though this was also observed to be the case for the Mean Absolute Error (MAE) index values, yet the analysis revealed that the overall MAE values for both seasons (Rabi 2013-14 and Rabi 2018-19) put together were significantly

**Table 4: Catchment scale mean observed vs. predicted ETa of the agricultural areas in Narmada Canal Project during (2018-19) Rabi season**

| Date       | Crop Growth Stage | GLDAS_ET0 | Kc   | GLDAS_ETa | EEFlux ETa (mm/d) |          | SETMI Ea (mm/d) |          |
|------------|-------------------|-----------|------|-----------|-------------------|----------|-----------------|----------|
|            |                   |           |      |           | mean              | $\sigma$ | mean            | $\sigma$ |
| 24/11/2018 | Initial           | 4.02      | 0.4  | 1.61      | 0.92              | 0.74     | 2.21            | 0.67     |
| 26/12/2018 | Vegetative        | 3.56      | 1.12 | 3.99      | 1.4               | 0.92     | 1.81            | 0.66     |
| 11/01/2019 | Mid-season        | 3.77      | 1.14 | 4.30      | 1.05              | 0.36     | 1.86            | 0.74     |
| 27/01/2019 | Late-season       | 3.81      | 1.1  | 4.19      | 2.43              | 1.47     | 1.88            | 0.83     |
| 28/02/2019 | Late-season       | 4.80      | 0.4  | 1.92      | 1.72              | 0.85     | 1.4             | 0.63     |

**Table 5: Values of agreement indices for computing model performance**

| Statistical Indices | Rabi Period 2013-14 |       | Rabi Period 2018-19 |       | Both Seasons Pooled |       |
|---------------------|---------------------|-------|---------------------|-------|---------------------|-------|
|                     | EEFlux              | SETMI | EEFlux              | SETMI | EEFlux              | SETMI |
| RMSE (mm/d)         | 0.64                | 1.17  | 2.04                | 1.83  | 1.58                | 1.57  |
| MAE (mm/d)          | 0.54                | 1.14  | 1.70                | 1.61  | 1.18                | 1.40  |
| MBE (mm/d)          | 0.05                | -0.19 | 1.70                | 1.37  | 0.97                | 0.68  |
| NSE                 | 0.80                | 0.34  | -0.06               | 0.15  | 0.19                | 0.21  |
| d-index             | 0.95                | 0.78  | 0.29                | 0.31  | 0.63                | 0.55  |

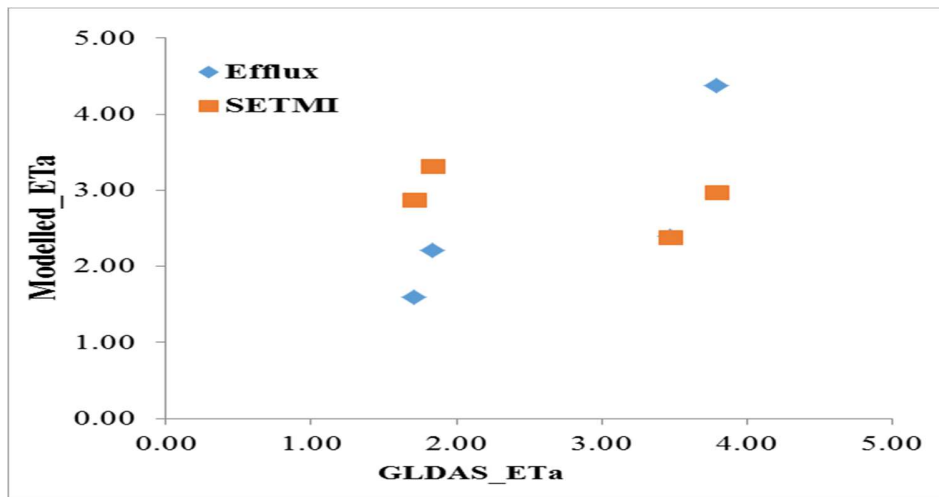


**Figure 7: Observed versus predicted actual evapotranspiration (ETa) for Rabi season of 2013-14**

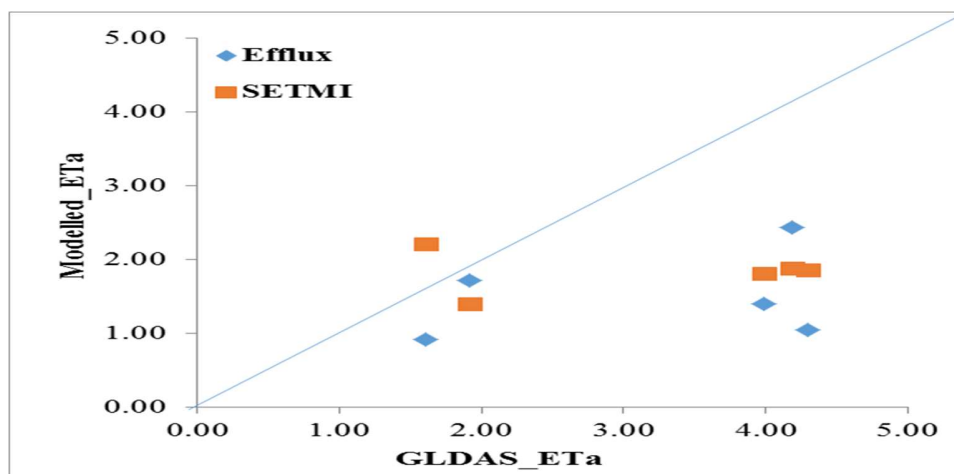


**Figure 8: Observed versus predicted actual evapotranspiration (ETa) for Rabi season of 2018-19**

lower for the EEFlux model (1.18 mm/d) than the SETMI model (1.40 mm/d). Further, though the EEFlux model was observed to be associated with somewhat higher bias than the SETMI model (as evident from the statistics on the pooled data in last two column of the row illustrating MBE index values under Table 5) yet the pooled Nash-Sutcliffe Efficiency index (NSE) and the index of agreement (d-index) values for the two approaches appeared to be quite comparable, with EEFlux modelling approach having a visible edge over the SETMI modelling approach particularly during 2013-14 Rabi season.

The investigations thus illustrated at par performance of both EEFlux and SETMI models in the arid region of the Narmada Canal Project of Rajasthan, India and thereby re-iterated that it's not necessary that a more detailed two-source surface energy balance approach, capable of computing surface energy balance of heterogeneous surfaces with greater accuracy, be outperforming a simple single-source model under all situations (Kustas and Norman, 1996; Troufleau *et al.*, 1997; Bastiaanssen *et al.*, 1998). In fact, our experience revealed that the dual source, SETMI modelling approach required more careful model input data parameterization, especially with respect to the target area's land use and crop coefficient values, as compared to the EEFlux model where the same were completely automated thereby decreasing the negative impacts of the inferior user skill set or user-errors on the quality of the generated model inputs and thus model-reproducibility in terms of its outputs or performance. These results were observed to be in close conformity with even those obtained by French, *et al.* (2015), Timmermanns, *et al.* (2007) and Liaqat and Choi (2015). Thus, the present study strongly recommended the use of single-source surface energy balance approach namely EEFlux particularly for the arid regions of the developing nations, where limited data availability and computational resource pose significant challenges.

## References

Allen, R. G., Pereira, L. S., Raes, D. & Smith, M. (1998). Crop Evapotranspiration – Guidelines for Computing Crop Water Requirements. *FAO Irrigation and Drainage Paper 56*. Rome, Italy: Food and Agriculture Organization of the United Nations (FAO).  
<https://www.fao.org/3/X0490E/x0490e00.htm>.

## Conclusion

Remote sensing-based single and dual-source surface energy balance modeling approaches represent cutting-edge techniques for operationalizing actual evapotranspiration-based demand driven irrigation systems. Normally the more detailed dual-source surface energy balance approaches are assumed to be superior to the simpler single-source energy balance modelling approaches. However, the present investigation, that was primarily aimed at assessing the comparative performance efficiency of the single-source, EEFlux and the dual-source, SETMI models for estimating actual evapotranspiration flux over the Narmada Canal Command area of the arid Rajasthan state of India, clearly showed that the afore-stated assumption need not be universally applicable as in the present investigation the test single source model namely, EEFlux seemed to be performing at par with the dual source, SETMI model. In fact, the present study demonstrated distinct advantages of the single source EEFlux model over the dual source SETMI model due to its user friendly, automated implementation and low input data requirements thereby making it the most suitable approach for particularly the resource crunched and vulnerable arid regions of the world having limited input data and computational resources.

## Acknowledgement

The authors are thankful to the United States India Educational Foundation funded US - India 21<sup>st</sup> Century Knowledge Initiative program on “*Improving water management, agricultural production and food security in drought prone areas*” under which this investigation was carried out.

## Conflict of interest

The authors declare that they have no conflict of interest.

Allen, R. G., Tasumi, M. & Trezza, R. (2007). Satellite-based energy balance for mapping evapotranspiration with internalized calibration (METRIC) model. *Journal of Irrigation and Drainage Engineering*, 133, 380-394.  
[https://doi.org/10.1061/\(ASCE\)0733-437\(2007\)133:4\(380\)](https://doi.org/10.1061/(ASCE)0733-437(2007)133:4(380)).

- Allen, R. G., Morton, C., Kamble, B., Kilic, A., Huntington, J., Thau, D., Gorelick, N., Erickson, T., Moore, R., Trezza, R., Ratcliffe, I. & Robison, C. (2015). EEFlux: a landsat based evapotranspiration mapping tool on the google earth engine. In: *American Society of Agricultural and Biological Engineers irrigation symposium: Emerging Technologies for Sustainable Irrigation* (pp: 1-11), Long Beach, California USA. [doi:10.13031/irrig.20152143511](https://doi.org/10.13031/irrig.20152143511).
- Bastiaanssen, W. G. M., Pelgrum, H., Wang, J., Ma, Y., Moreno, J. F., Roerink, G. J. & Van der Wal, T. (1998). A remote sensing surface energy balance algorithm for land (SEBAL). Part 2: Validation. *Journal of Hydrology*, 212-213, 213-229. [https://doi.org/10.1016/S0022-1694\(98\)00254-6](https://doi.org/10.1016/S0022-1694(98)00254-6).
- Courault, D., Seguin, B. & Olioso, A. (2005). Review on estimation of evapotranspiration from remote sensing data: From empirical to numerical modeling approaches. *Irrigation and Drainage Systems*, 19, 223-249. <https://doi.org/10.1007/s10795-005-5186-0>.
- Dai, L., Fu, R., Zhao, Z., Guo, X., Du, Y., Hu, Z. & Cao, G. (2022). Comparison of fourteen reference evapotranspiration models with lysimeter measurements at a site in the humid alpine meadow, Northeastern Qinghai-Tibetan plateau. *Frontiers in Plant Science*, 13, 854196. <https://doi.org/10.3389/fpls.2022.854196>.
- French, A. N., Hunsaker, D.J. & Thorp, K. R. (2015). Remote sensing of evapotranspiration over cotton using the TSEB and METRIC energy balance models. *Remote Sensing of Environment*, 158, 281-294. <https://doi.org/10.1016/j.rse.2014.11.003>.
- Geli, H. M. E. & Neale, C. M. U. (2012). Spatial Evapotranspiration Modelling Interface (SETMI). *Remote Sensing and Hydrology*, 352, 171-174. <http://www.scopus.com/inward/record.url?scp=84883427838&partnerID=8YFLogxK>.
- Gowda, P. H., Chávez, J. L., Howell, T. A., Marek, T. H. & New, L. L. (2008). Surface energy balance-based evapotranspiration mapping in the Texas high plains. *Sensors*, 8, 5186-5201. <https://doi.org/10.3390/s8085186>.
- Huntingford, C., Verhoef, A. & Stewart, J. (2000). Dual versus single source models for estimating surface temperature of African savannah. *Hydrology and Earth System Sciences*, 4(1), 185-191. [10.5194/hess-4-185-2000](https://doi.org/10.5194/hess-4-185-2000).
- Kool, D., Agam, N., Lazarovitch, N., Heitman, J. L., Sauer, T. J. & Ben-Gal, A. (2014). A review of approaches for evapotranspiration partitioning. *Agricultural and forest meteorology*, 184, 56-70. <https://doi.org/10.1016/j.agrformet.2013.09.003>.
- Kushwaha, N. L., Rajput, J., Sena, D. R., Elbeltagi, A., Singh, D. K. & Mani, I. (2022). Evaluation of data-driven hybrid machine learning algorithms for modelling daily reference evapotranspiration. *Atmosphere-Ocean*, 60(2), 1-22.
- Kustas, W. P. & Norman, J. M. (1996). Use of remote sensing for evapotranspiration monitoring over land surfaces. *Hydrological Sciences Journal*, 41(4), 495-516. <https://doi.org/10.1080/02626669609491522>.
- Liaquat, U. W. & Choi, M. (2015). Surface energy fluxes in the Northeast Asia ecosystem: SEBS and METRIC models using Landsat satellite images. *Agricultural and Forest Meteorology*, 214-215, 60-79. <https://doi.org/10.1016/j.agrformet.2015.08.245>.
- Li, Z. L., Tang, R., Wan, Z., Bi, Y., Zhou, C., Tang, B., Yan, G. & Zhang, X. (2009). A review of current methodologies for regional evapotranspiration estimation from remotely sensed data. *Sensors*, 9, 3801-3853. <https://doi.org/10.3390/s90503801>.
- Liou, Y. A. & Kar, S. K. (2014). Evapotranspiration estimation with remote sensing and various surface energy balance algorithms-A review. *Energies*, 7(5), 2821-2849. <https://doi.org/10.3390/en7052821>.
- Merlin, O. & Chehbouni, A. (2004). Different approaches in estimating heat flux using dual angle observations of radiative surface temperature. *International Journal of Remote Sensing*, 25(1), 275-289. <https://doi.org/10.1080/0143116031000116408>.
- Moriassi, D. N., Arnold, J. G., Van Liew, M. W., Bingner, R. L., Harmel, R. D. & Veith, T. L. (2007). Model evaluation guidelines for systematic quantification of accuracy in watershed simulations. *Transactions of the ASABE*, 50(3), 885-900. <https://doi.org/10.13031/2013.23153>.
- Nash, J. E. & Sutcliffe, J. V. (1970). River flow forecasting through conceptual models' part 1- A discussion of principles. *Journal of Hydrology*, 10(3), 282-290. [https://doi.org/10.1016/0022-1694\(70\)90255-6](https://doi.org/10.1016/0022-1694(70)90255-6).
- Neale, C. M. U., Bausch, W. C. & Heerman, D. F. (1989). Development of Reflectance- Based Crop Coefficients for Corn. *Transactions of the American Society of Agricultural Engineers*, 32(6), 1891-99. <https://doi.org/10.13031/2013.31240>.
- Neale, C. M. U., Geli, H. M. E., Kustas, W. P., Alfieri, J. G., Gowda, P. H., Evett, S. R., Prueger, J. H., Hipps, L. E., Dulaney, W. P., Chavez, J. L., French, A. N. & Howell, T. A. (2012). Soil water content estimation using a remote sensing-based hybrid evapotranspiration modeling approach. *Advances in Water Resources*, 50, 152-161. <https://doi.org/10.1016/j.advwatres.2012.10.008>.
- Norman, J. M., Kustas, W. P. & Humes, K. S. (1995). Source Approach for Estimating Soil and Vegetation Energy Fluxes in Observations of Directional Radiometric Surface Temperature. *Agricultural and Forest Meteorology*, 77(3-4), 263-93. [https://doi.org/10.1016/0168-1923\(95\)02265-Y](https://doi.org/10.1016/0168-1923(95)02265-Y).

- Norman, J. M., Kustas, W. P., Preuger, J. H. & Diak, G. R. (2000). Surface flux estimation using radiometric temperature: a dual-temperature-difference method to minimize measurement errors. *Water Resources Research*, 36, 2263-2274. <https://doi.org/10.1029/2000WR900033>.
- Saha, S., Moorthi, S., Pan, H., Wu, X., Wang, J., Nadiga, S., Tripp, P., Kistler, R., Woollen, J., Behringer, D. & coauthors. (2010). The NCEP Climate Forecast System Reanalysis. *Bulletin of the American Meteorological Society*, 91, 1015-1058. <https://doi.org/10.1175/2010BAMS3001.1>.
- Saha, S., Moorthi, S., Wu, X., Wang, J., Nadiga, S., Tripp, P., Behringer, D., Hou, Y., Chuang, H., Iredell, M. & coauthors. (2013). The NCEP Climate Forecast System Version 2. *Journal of Climate*, 27, 2185-2208. <https://doi.org/10.1175/JCLI-D-12-00823.1>.
- Salam, R., Islam, A. R. M. T., Pham, Q. B., Dehghani, M., Al-Ansari, N. & Linh, N. T. T. (2020). The optimal alternative for quantifying reference evapotranspiration in climatic sub-regions of Bangladesh. *Science and Reports*, 10(1), 20171. <https://doi.org/10.1038/s41598-020-77183-y>.
- Singh, R. K., Irmak, A., Irmak, S. & Martin, D. L. (2008). Application of SEBAL Model for Mapping Evapotranspiration and Estimating Surface Energy Fluxes in South-Central Nebraska. *Journal of Irrigation and Drainage Engineering*, 134(3), 273-285. [https://doi.org/10.1061/\(ASCE\)0733-9437\(2008\)134:3\(273\)](https://doi.org/10.1061/(ASCE)0733-9437(2008)134:3(273))
- Teixeira, A. H. D. C., Bastiaanssen, W. G. M., Ahmadd, M. D. & Bos, M. G. (2009). Reviewing SEBAL input parameters for assessing evapotranspiration and water productivity for the Low-Middle São Francisco River basin, Brazil Part A: Calibration and validation. *Agricultural and Forest Meteorology*, 149, 462-476. <https://doi.org/10.1016/j.agrformet.2008.09.016>.
- Timmermans, W.J., Kustas, W.P., Anderson, M.C. & French, A. N. (2007). An intercomparison of the Surface Energy Balance Algorithm for Land (SEBAL) and the Two-Source Energy Balance (TSEB) modeling schemes. *Remote Sensing of Environment*, 108(4), 369-384. <https://doi.org/10.1016/j.rse.2006.11.028>.
- Troufleau, A. D., Lhomme, J., Monteny, B. & Vidal, A. (1997). Sensible heat flux and radiometric surface temperature over sparse sahelian vegetation. I. An experimental analysis of the  $kB^{-1}$  parameter. *Journal of Hydrology*, 188-189, 815-838. [https://doi.org/10.1016/S0022-1694\(96\)03172-1](https://doi.org/10.1016/S0022-1694(96)03172-1).
- Verhoef, A., McNaughton, K. G. & Jacobs, A. F. G. (1997). A parameterization of momentum roughness length and displacement height for a wide range of canopy densities. *Hydrology and Earth System Sciences*, 1(1), 81-91. <https://doi.org/10.5194/hess-1-81-1997>.
- Vorosmarty, C., McIntyre, P., Gessner, M., Dudgeon, D., Prusevich, A., Green, P., Glidden, S., Bunn, S., Sullivan, C., Liermann, C. & Davies, P. (2010). Global threat to human water security and river biodiversity. *Nature*, 467(7315), 555-561. <https://doi:10.1038/nature09440>.
- Wang, K. & Dickinson, R. E. (2012). A review of global terrestrial evapotranspiration: Observation, modeling, climatology, and climatic variability. *Reviews of Geophysics*, 50(2), 1-54. <https://doi.org/10.1029/2011RG000373>.
- Yuan, X., Wood, E. F., Luo, L. & Pan, M. (2011). A first look at Climate Forecast System version 2 (CFSv2) for hydrological seasonal prediction. *Geophysical Research Letters*, 38(13), 1-7. <https://doi.org/10.1029/2011GL047792>.
- Zhang, K., Kimball, J. S. & Running, S. W. (2016). A review of remote sensing based actual evapotranspiration estimation. *Wiley Interdisciplinary Reviews: Water*, 3(6), 834-853. <https://doi.org/10.1002/wat2.1168>.

**Publisher's Note:** ASEA remains neutral with regard to jurisdictional claims in published maps and figures.